Host genotype and colonist arrival order jointly govern plant microbiome composition and function

Devin R. Leopold[1*] & Posy E. Busby[1]

Department of Botany and Plant Pathology, Oregon State University, Corvallis, OR, 97331, USA

[*]Correspondence: devin.leopold@gmail.com

Summary

The composition of host-associated microbiomes can have important consequences for host health and fitness [1–3]. Yet, we still lack understanding of many fundamental processes that determine microbiome composition [4,5]. There is mounting evidence that historical contingency during microbiome assembly may overshadow more deterministic processes, such as the selective filters imposed by host traits [6–8]. More specifically, species arrival order has been frequently shown to affect microbiome composition [9–12], a phenomenon known as priority effects [13–15]. However, it is less clear whether priority effects during microbiome assembly are consequential for the host [16], or whether intraspecific variation in host traits can alter the trajectory of microbiome assembly under priority effects. In a greenhouse inoculation experiment, using the black cottonwood (*Populus trichocarpa*) foliar microbiome, we manipulated host genotype and the colonization order of common foliar fungi. We quantified microbiome assembly outcomes using fungal marker-gene sequencing and measured susceptibility of the colonized host to a leaf rust pathogen, *Melampsora* × *columbiana*. We found that the effect of species arrival order on microbiome composition, and subsequent disease susceptibility, depended on the host genotype. Additionally, we found that microbiome assembly history can affect host disease susceptibility independent of microbiome composition at the time of pathogen exposure, suggesting that the interactive effects of species arrival order and host genotype can decouple composition and function in the plant microbiome. Overall, these results highlight the importance of a key process underlying stochasticity in microbiome assembly while also revealing which hosts are most likely to experience these effects.

Keywords: community assembly; community ecology; endophyte; foliar fungi; historical contingency; *Populus trichocarpa*; priority effects; plant microbiome

RESULTS AND DISCUSSION

In this study, we sought to determine whether intraspecific variation in the model tree species, *Populus trichocarpa*, and the inoculation order of non-pathogenic foliar fungi interactively determine foliar microbiome composition and plant disease susceptibility. Specifically, we conducted a greenhouse experiment using 12 clonally propagated *P. trichocarpa* genotypes and a synthetic community of 8 common foliar fungi, which were isolated from field collected *P. trichocarpa* leaves. The plant genotypes can be broadly classified into two ecotypes, eastern and western, originating from either side of the Cascade Range that bisects the tree's native range in Northwestern North America (Figure S1). The mountains create a sharp transition from a wet and mild environment in the west, to a dry continental environment in the east. The *P. trichocarpa* ecotypes associated with these regions vary in leaf morphology [17], foliar disease susceptibility [18–20], and are exposed to distinct microbial species pools [21]. Because these characteristics define the physical environment of the foliar microbiome (i.e., the leaf) [22,23] and suggest differences in innate immune responses to microbial colonization [24,25], we expected to observe the largest differences in host effects on foliar microbiome assembly when comparing eastern and western ecotypes.

Fungal species composition in the P. trichocarpa foliar microbiome depends on both species arrival order and host genotype.

We first sought to test the hypothesis that the effect of species arrival order on the relative abundance of foliar fungi would vary among *P. trichocarpa* genotypes and ecotypes. We created 5 immigration history treatments in which one member of our 8-species synthetic community was allowed to preemptively colonize leaves, followed by inoculation with the full community 2 weeks later. We assessed fungal community assembly outcomes using marker-gene sequencing and modeled variation in species relative abundances (Figure 1a) using joint-species distribution models [26], accounting for taxon-specific sequencing biases using empirical estimates derived from mock-community data (Figures S2).

At the community-level, we found that fungal species composition depended on species arrival order (Wald-$\chi^2_{(4)}$ = 21.8, $P < 0.001$; Figure 1c), and that the effect of arrival order varied across plant genotypes (Wald-$\chi^2_{(44)}$ = 23.5, $P = 0.04$; Table S2). The direct effect of plant genotype on

fungal species composition (Wald-$\chi^2_{(11)}$ = 20.2, $P < 0.001$) was partially explained by host ecotype (Wald-$\chi^2_{(1)}$ = 12.4, $P < 0.001$; Figures 1a & 1d). However, contrary to our expectations, we did not find evidence to support the hypothesis that the effect of species arrival order on fungal community composition is systematically influenced by host ecotype (Wald-$\chi^2_{(4,238)}$ = 6.16, $P = 0.31$; Table S2). This suggests that the plant traits that interact with species arrival order to affect community assembly are not the physical leaf traits that broadly segregate across the wet and dry regions sampled. It is possible that other traits with greater variance among individual *P. trichocarpa* genotypes, such as those involved in microbial recognition and immune response signaling [27–29], are responsible for the genotype-by-arrival order interaction we observed. However, experiments across many more genotypes, using genome wide association analyses, would be needed to test this hypothesis [30].

Community-level variation in fungal species composition was the result of differing responses of individual fungi to the experimental design, with some species responding more strongly to arrival order and others responding more strongly to host genotype (Figure 1b). The effect of species arrival order was not limited to taxa that served as initial colonists, indicating that the identity of the initial colonist can result in complex indirect effects on the trajectory of community assembly. However, when the relative abundances of individual species were analyzed independently we did not find strong evidence that the effect of species arrival order varied among host genotypes; an effect that only became evident for the community as a whole.

The advantage of preemptive colonization depends on species identity and host genotype, but not host ecotype.

Variation in the identity of the initial colonist affected the relative abundances of all but one member of the synthetic community of foliar fungi, yet, only 3 of the 5 early arriving species consistently experienced a benefit from preemptive colonization (Figure 2). This could be the result of intrinsic fitness differences among the initial colonists, or differences in their niche overlap with the other community members, affecting the benefit of early arrival [31,32]. For example, *Alternaria* had the greatest relative abundance across all treatments and, although it did benefit from early arrival, the magnitude of the observed priority effect for this species was relatively low. This could suggest that *Alternaria* is competitively dominant within the foliar

microbiome, limiting the possibility of niche preemption by other species, though we cannot rule out the possibility that this species occupies a distinct niche within the leaf. Niche differences, such as specialization on the leaf surface vs. interstitial space would also reduce the relative importance of arrival order and could explain why species that did not benefit from early arrival often varied in relative abundance in response to the identity of other initial colonists.

Because the synthetic communities used in this experiment all included the same 8 fungal species, yet natural plant microbiomes can host hundreds species [33,34], it is likely that our experimental design represents a conservative test for the strength of priority effects. Priority effects are more likely to be strong when the pool of potential colonists is larger because greater niche overlap and niche modification are both more likely [35]. In addition, our immigration history treatments involved applying just one third of the total inoculum of one species initially, with the remainder applied concurrent with the other community members. This was done to ensure that any observed effects were the result of preemptive colonization and not differences in total quantity of inoculum or absence of the initial colonist from the community inoculum applied later. As a result, our assembly history perturbations were relatively subtle compared to the potential stochasticity that can result from dispersal processes occurring in natural microbial communities [36].

Foliar microbiome assembly history affects rust disease severity in susceptible plant genotypes

To test the hypothesis that foliar disease severity depends on the joint effects of host genotype and species arrival order during foliar microbiome assembly, we inoculated plants with the leaf rust pathogen, *Melampsora* × *columbiana*, 2 weeks after establishing foliar microbiomes under our immigration history treatments. We then used image analysis to quantify disease severity as the proportion of leaf area that developed chlorotic lesions and used beta-regression models to assess variation across treatments (Figure 3 & Table S3). As expected, the primary source of variation in rust disease severity was host ecotype, likely reflecting the presence of major-gene resistance to the rust pathogen in most, but not all, western genotypes (Figures 3 & S3).

We found that the effect of fungal species arrival order on rust disease severity depended on whether the host genotype was susceptible or resistant to the rust pathogen. Specifically, for susceptible, primarily eastern genotypes, disease severity depended on the interaction between

fungal species arrival order and host genotype (LRT-$\chi^2_{(20)}$ = 33.6, P = 0.03; Figure 3a). However, while there was variation in the overall level of rust disease observed among the highly rust resistant, western genotypes (LRT-$\chi^2_{(5)}$ = 33.5, P < 0.001; Figure 3b), the arrival order of foliar fungi did not affect rust disease development (LRT-$\chi^2_{(20)}$ = 1.74, P = 0.78).

Although we found that microbiome assembly history affected subsequent disease severity in rust susceptible plant genotypes, we did not find evidence that this was the result of consistent shifts in the relative abundance of individual fungi or the overall shifts in foliar microbiome composition (Figure S4). One explanation for this could be that disease modification by early arriving species occurred primarily through interaction with the plant's immune system [37,38], decoupling the outcome of microbiome community assembly from disease development. Alternatively, disease modification may be the result of complex direct and indirect interactions with the entire fungal community, not individual species. Although some individual foliar fungi can have large effects on *P. trichocarpa* foliar rust severity [39], we did not pre-screen the fungi to select species that were associated with disease modulation effects. Including such species in our synthetic communities may have yielded stronger links between fungal community composition and rust disease.

Standard approaches for marker-gene sequencing of microbiome communities only provide data on the relative abundances of taxa within each sample, i.e., compositional data [40,41]. It is possible that total fungal abundance in the foliar microbiome varies among plant genotypes due to variation in resource availability, leaf thickness, or other leaf traits [42]. Variation in total fungal abundance could be consequential for disease modulation, particularly if direct pathogen antagonism by non-pathogenic microbes contributes to disease suppression. Variation in total microbial abundance could also have implications for priority effects during microbiome community assembly. Specifically, priority effects should be more important when the community size is limited by space or resources because niche preemption by early arriving species is more likely [43,44]. However, priority effects may be stronger in resource rich environments if the growth rate of early arriving species is increased [45,46], though greater local resource availability can reduce the strength of priority effects in some fungi by reducing the rate of substrate exploration [47]. Progress towards understanding the interactive effects

species arrival order and host genotype on plant microbiome composition and function will require quantitative data on microbial abundance.

Conclusions

In a recent study, Carlström *et al.* [11] used experimental manipulations of a synthetic community of *Arabidopsis thaliana* phyllosphere bacteria to demonstrate that colonization timing has important consequences for community assembly outcomes in the foliar microbiome. Here, we have shown that host genotype and species arrival order interact to determine the trajectory of microbiome community assembly. This finding suggests that the effects of species arrival order and timing are mediated by host traits, and that future efforts should aim to identify these traits to work towards truly generalizable microbiome community assembly rules. We additionally show that the disease modulation function of the foliar microbiome can be affected by species arrival order, and that this effect may be decoupled from microbiome composition. This finding raises intriguing questions about the direct and indirect interaction networks that may underlay disease modulation by foliar fungi. Addressing these complex questions will require novel computational approaches that merge the multiple layers of omics networks that are increasingly available for model plants, such as *P. trichocarpa* [e.g., 48]. Finally, our study has demonstrated the feasibility of controlled manipulations of fungal community assembly in the phyllosphere using a tractable synthetic community. While manipulations of synthetic plant microbiomes is increasingly seen as a valuable experimental approach, most efforts have focused on bacteria [49,50], while fungi are often the most functionally prominent symbionts associated with plants [51]. Future manipulative experiments using synthetic fungal communities will be necessary to establish the foundational knowledge needed to realize the promise of selective manipulation of plant microbiome assembly for applications in agriculture or natural resource management.

ACKNOWLEDGMENTS

We are grateful to Bruce McCune, George Newcombe, Maggie Wagner, and Timothy Warren for feedback during the preparation of this manuscript. This research was supported by the US Department of Energy's Office of Biological and Environmental Research (DE-SC0019435) and by the Oregon State University, Department of Botany and Plant Pathology.

AUTHOR CONTRIBUTIONS

DRL and PEB jointly planned the study. DRL lead implementation, data collection, analysis, and manuscript preparation, with input and contributions from PEB at all stages.

DECLARATION OF INTERESTS

The authors declare no competing interests.

FIGURE LEGENDS

Figure 1: *Fungal species composition in the foliar microbiome depends on both species arrival order and host genotype*.

(a) Heatmap shows standardized variation in fungal relative abundance for each species, with species arranged from the most to least abundant, top to bottom (rows). Individual panels show the 5 immigration history treatments, labeled with identity of the initial colonist. Cells showing the relative abundance of the initial colonist in each immigration history treatment are highlighted. Columns represent individual eastern or western *P. trichocarpa* genotypes, and columns within each panel have been sorted using non-metric multidimensional scaling of community dissimilarity.

(b) Results of univariate models of individual species relative abundances, testing the joint effects of species arrival order treatments (T), host genotype (G), and host ecotype (E). Colors indicate the partial *pseudo-*r^2 for each model term, calculated following the method of Nagelkerke [52]. Symbols indicate the significance (permutation tests) of individual species' contributions to the multivariate (community-level) response, calculated using step-down resampling to account for multiple testing, where $^{+}P < 0.1$, $^{*}P < 0.05$, $^{**}P < 0.01$, and $^{***}P < 0.001$.

(c) Distance-based redundancy analysis, showing variation in fungal community dissimilarity (Jensen-Shannon distance) among initial colonist treatments after conditioning on the effect of host genotype. Colored points show the group means (± sd) for initial colonist treatments on the first 2 constrained axes.

(d) Distance-based redundancy analysis, showing variation in fungal community dissimilarity (Jensen-Shannon distance) among host genotypes after conditioning on the effect of the initial

colonist treatments. Colored points show the group means (± sd) for each plant genotype on the first 2 constrained axes and color indicate host ecotype.

Figure 2: *The advantage of preemptive colonization in the foliar microbiome depends on species identity and host genotype, but not host ecotype.*
The strength of priority effects for each species on each genotype was calculated as the log ratio of the relative abundance when arriving first vs. arriving concurrent with the community. Points show the estimated priority effect for each fungal species (panels) on each plant genotype (point colors) and error bars indicate 95% bootstrapped confidence intervals. Insets show bootstrap distributions of the mean strength of priority effects for the eastern and western *P. trichocarpa* ecotypes. Significant mean priority effects, based on bootstrapped one-sample t-tests, are indicated, where $^{*}P < 0.05$, $^{**}P < 0.01$, and $^{***}P < 0.01$.

Figure 3: *Foliar microbiome assembly history affects rust disease severity in susceptible plant genotypes.*
Large points indicate the estimated marginal means (± 95% CIs) from beta-regression models of disease severity in leaf rust (a) susceptible and (b) resistant *P. trichocarpa* genotypes. Small points show individual rust severity observations (% leaf area with chlorotic lesions) for each species arrival order treatment (colors) on each host genotype (panels). Transparency of small points indicates the weight used (number of individual leaves measured per plant) in the beta-regression models. Horizontal dotted lines indicate the mean rust severity in uninoculated control plants.

METHODS

Overview and experimental design

We manipulated the species arrival order of foliar fungi colonizing the leaves of 12 genotypes of the model tree species, *P. trichocarpa*, in a controlled greenhouse experiment. The plant genotypes originated from populations located both east (5) and west (7) of the Cascade Divide in the northwestern United States (Figure S1). In the greenhouse, plants were inoculated with a synthetic community of 8 fungal species (Table S1), all isolated from field collected *P. trichocarpa* leaves. Inoculation consisted of two phases: colonization by 1 of 5 randomly selected initial colonists, followed 2 weeks later by inoculation with the full synthetic fungal

community. The 5 inoculation treatments, and an additional non-inoculated control treatment, were applied to 5 replicates of 12 clonally propagated *P. trichocarpa* genotypes, resulting in a total of 360 plants. We assessed fungal community assembly outcomes after one month using Illumina sequencing of the nuclear ribosomal, internal transcribed spacer (ITS) region. We then inoculated plants with the foliar rust pathogen *Melampsora* × *columbiana* and assessed disease severity to quantify functional consequences of priority effects in the *P. trichocarpa* foliar microbiome.

Plant propagation

Plants were propagated in a glasshouse on the campus of Oregon State University using dormant hardwood cuttings collected in February 2018, from a common garden. Cuttings were trimmed to *ca.* 10 cm and planted into 550 ml conical Deepots (Stuewe & Sons, Inc.) using commercial potting mix (Sunshine Mix #4) supplemented with 115 ml gal^{-1} slow-release fertilizer (16-6-11+micronutrients). Throughout the experiment, plants were watered from below using an automated sub-irrigation system to keep leaves dry and limit opportunities for colonization by non-target fungi [53].

Synthetic fungal community

We isolated foliar fungi from *P. trichocarpa* leaves using standard methods. Briefly, leaf punches were collected into sterile 1.5 ml centrifuge tubes and surface sterilized by sequentially vortexing for 1 minute in 10% bleach (0.825% NaClO), 70% EtOH, and then in 3 consecutive rises in sterile water. We then plated the leaf punches onto potato-dextrose agar, supplemented with penicillin (100 μg ml^{-1}) and streptomycin (100 μg ml^{-1}), and incubated the plates at room temperature for 1 month. Plates were checked daily for fungal growth and emerging hyphae were subcultured using single hyphal-tip isolation. We selected representative morphotypes from the initial culture collection and used Sanger sequencing of the full ITS region for taxonomic identification. We then selected representative isolates of 8 fungal species (Table S1) to use in our synthetic community of *P. trichocarpa* foliar fungi, which included: *Alternaria alternata*, *Aureobasidium pullulans*, *Cladospoium* sp., *Dioszegia butyracea*, *Epicoccum nigrum*, *Fusarium* sp., *Penicillium bialowiezense*, and *Trichoderma trixiae*. The isolates we selected have been previously identified as common members of the *P. trichocarpa* foliar microbiome [21,39]. Because definitive species-level identifications from ITS sequence data is not always possible,

the genus-level taxonomic assignments will be used to refer to the individual isolates hereafter. Sanger sequences of the full ITS region for the 8 focal species are archived in the NCBI genbank (accession numbers MT035960-7).

Fungal inoculation

We collected fungal inoculum by flooding 2-week old cultures with an aqueous solution of 0.1% Tween 20 and gently scraping the plate surface with a sterile spatula to dislodge conidia, or, in the cases of the yeast-like *Aureobasidium pullans* and the basideomycetous yeast, *Dioszegia* sp., individual cells. We quantified the density of the initial suspension using a hemocytometer and diluted as required using additional sterile 0.1% Tween 20. At the first inoculation time point, we prepared inoculation solutions for each of the 5 initial colonists at a density of 3.3×10^4 cells ml^{-1}. At the second time point, 2 weeks later, inoculation solutions for each treatment were prepared containing each of the 7 other species at a density of 1.0×10^5 cells ml^{-1} and the initial colonist at a density of 6.7×10^4 cells ml^{-1}. As a result, the total amount of inoculum for each species in each treatment was held constant and only the identity of the initial colonist varied. We chose to apply the majority of the inoculum for the initial colonist at the second time point to ensure that differences in assembly outcomes were due to early arrival, and not the absence of the initial colonist from the inoculation solution during colonization by the full community.

Inoculation of plants was achieved by saturating both the top and bottom leaf surfaces with a sterile, fine-mist spray bottle. For each tray holding 12 plants, we applied 75 ml of the inoculum solution and then immediately covered the tray with a temporary humidity tent to maintain leaf surface moisture for 48 hours. Control plants were mock-inoculated using sterile water at both time points. Because *P. trichocarpa* grows rapidly and the experiment was conducted over a period of 6 weeks, we used a wire twist tie to mark the youngest fully expanded leaf at the time of the first inoculation.

Leaf sampling for fungal DNA

From each plant, we collected 4 leaf punches (*ca*. 0.25 cm^2) from each of 3 leaves (12 total) directly into a sterile 1.5 ml centrifuge tube using a standard hole punch, which was cleaned with ethanol between each plant. Leaf disks were placed on ice immediately after collection and processed to remove surface contaminants the same day they were collected. To remove surface

contaminants, the leaf disks were agitated for 1 minute in 1 ml of molecular grade water with 0.1% Tween 20, using a Geno/Grinder® 2010, set at 500 strokes per minute. The cleaning solution was remove from the tubes using a sterile pipette and the leaf disks were rinsed by repeating the process 3 times with molecular grade sterile water. The cleaned leaf disks were then frozen at -20 °C and stored until we extracted total genomic DNA using the 96 Well Synergy™ Plant DNA Extraction Kit (OPS Diagnostics). The four corners of each extraction plate were processed without leaf disks to serve as negative controls during library preparation.

Library preparation for ITS metabarcoding

We prepared libraries for Illumina MiSeq metabarcoding, targeting the ITS1 region using a dual-indexed, two-stage PCR approach. In the first PCR, we used modified versions the fungal specific forward gene primer ITS1F [54] and, for the reverse gene primer, the reverse-complement of gITS7 [55]. Each gene primer was fused with Illumina sequencing primers, separated by a 3-6 bp, degenerate, length-heterogeneity spacer [56]. Stage-one PCR was carried out in 25 µl reactions with MyFi Master Mix (Bioline), 2 µl template DNA, 0.5 µM of each primer and a thermocycling program consisting of an initial denaturing and enzyme activation cycle at 95 °C (3 min.), 32 cycles of 95 °C (30 sec.), 50 °C (30 sec.), and 72 °C (30 sec.), followed by a final elongation cycle at 72 °C (5 min). Temperature ramp rates were limited to 1 °C [57]. For each 96-well plate, 2 extraction blanks were included to detect contaminants possibly introduced during DNA extraction and 2 PCR blanks, with no template DNA, were included to detect contamination introduced during library preparation. For stage-two PCR, we used primers that targeted the Illumina sequencing adapters added during stage-one, adding the P5 and P7 Illumina adapters and 8-mer multiplexing barcodes [58]. Multiplexing barcodes were selected to have a minimum Hamming distance of 4 and balanced base diversity [59]. Stage-two PCR was carried out in 20 µl reactions with MyFi Master Mix, 1 µl of the stage-one PCR product as template, 0.5 µM primers, and a thermocycler program consisting of an initial cycle of 95 °C (1 min.), 8 cycles of 95 °C (20 sec.), 55 °C (20 sec.), and 72 °C (30 sec.), followed by a final elongation cycle at 72 °C (5 min). Final PCR products were cleaned and normalized using Just-a-Plate, 96-well normalization and purification plates (Charm Biotech), then pooled and sent to the Oregon State University, Center for Genome Research and Biocomputing, for 250-bp, paired-end sequencing on the Illumina MiSeq platform.

Fungal community bioinformatics

Sequences were demultiplexed with Pheniqs v2.0.4 [60], using a phred-adjusted maximum likelihood confidence threshold of 0.995. Gene primers and length heterogeneity spacers were removed from the 5' ends of the paired reads using cutadapt v1.18 [61], discarding reads with gene primers not found in the expected positions. The 3' ends were trimmed to remove "read-through" adapter contamination using SeqPurge [62]. Following trimming, reads were filtered at a maximum expected error rate of 2 bp, denoised, and filtered of putative chimeras using DADA2 [63], with the expected amplicons for the 8 members of the synthetic community included as denoising priors to increase sensitivity. Denoised amplicons were then further collapsed to operational taxonomic units (OTUs) at 99% similarity using agglomerative, single-linkage clustering with the R-package DECIPHER [64] used to calculate pairwise dissimilarity. Host contamination was removed by filtering the resulting OTUs against the *P. trichocarpa* v3.0 genome [65] using Bowtie2 [66]. Other likely contaminants were filtered by removing OTUs whose prevalence or mean proportional abundance when present was greater in negative controls. Samples with less than 4000 sequences remaining after all filtering steps were removed from subsequent analyses. The final OTU-by-sample matrix and the sample metadata were combined in a single phyloseq object [67] for downstream manipulation and analysis in the R v3.6 statistical programming environment (R Core Team, 2019). The raw fastq sequence files are archived in the NCBI Sequence Read Archive (BioProject ID: PRJNA605581) and all bioinformatics scripts and sample meta data have been publicly archived (http://doi.org/10.5281/zenodo.3742666).

Rust disease severity

Immediately following leaf sampling for marker-gene sequencing, we inoculated plants with a rust pathogen. Asexual urediniospores were collected from a single-spore strain of *M.* × *columbiana* being maintained on *P. trichocarpa* plants in an isolated growth chamber. We applied urediniospores at a concentration of 1.0 x 10^4 ml^{-1}, following the same procedure described above. After 2 weeks, we harvested 3 leaves from each plant and photographed the abaxial surface from a fixed distance using a light box. We then used image analysis, with Fiji [68], to quantify rust disease severity. First, we isolated leaves from the image background and quantified total leaf area using color thresholding. We then used supervised image segmentation

[69] to quantify the proportion each leaf occupied by either chlorotic lesions or rust uredinia, to related measures of rust disease severity.

Estimating sequencing bias

To quantify and correct for species-specific sequencing biases introduced during Illumina library preparation and sequencing, we constructed mock communities with known abundances of fungal DNA that were sequenced along with our experimental samples. To assemble the mock communities, we first extracted genomic DNA from pure cultures of each of the 8 members of the synthetic community and the rust pathogen using the *Quick*-DNA Fungal/Bacterial Miniprep Kit (Zymo Research). We then used Sanger sequencing and Primer 3 [70] to design custom qPCR primers to quantify the concentrations of our pure culture extracts. We targeted the TEF1-α gene for qPCR quantification because it is a single-copy gene, unlike the ITS region, which can vary in copy number among fungi over several orders of magnitude [71], likely representing a large source of bias in fungal ITS metabarcoding. Absolute qPCR quantification was carried out using PowerUP SYBR Master Mix (Applied Biosystems) and the 7500 Fast Real-Time PCR System (Applied Biosystems). We then used the qPCR estimated concentrations of the single culture extracts to combine genomic DNA for each species in 10 different mock communities, each containing all 9 fungal species. For 1 mock community, all species were present in equal concentrations (5×10^4 copies μl^{-1}). For the remaining 9 mock communities, species were added at either, 1×10^4 copies μl^{-1}, 5×10^4 copies μl^{-1}, or 2.5×10^5 copies μl^{-1}. Each species was present at each concentration in 3 mock communities and all 9 mock communities had 3 species at each concentration. The resulting mock community samples were prepared for Illumina sequencing in parallel with the experimental samples following the protocol outlined above.

Sequencing read counts and the known proportional abundances of each species in each mock community were then used to estimate species-specific biases following the method of [72]. We found significant bias among the members of our mock communities (Figure S2), with *M.* x *columbiana*, having the greatest positive bias, being over represented relative to the most negatively biased species, *Penicillium* sp. by a factor of 40. Among the members of our synthetic community of foliar fungi, the most positively biased species was *Fusarium* sp., which was over represented relative to *Penicillium* sp. by a factor of 13. Use of the estimated bias correction factors to account for sequencing bias is described in the data analysis section below.

Data analysis

To assess whether the community assembly of *P. trichocarpa* foliar fungi was influenced by the 5 colonization order treatments, 12 host genotypes, and their interaction, we fit a multivariate, negative-binomial glm, using the R-package mvabund [73]. We accounted for 2 sources of unequal sampling effort, variable sampling depth and the species-specific sequencing biases, by including an offset term (*effort*) for each species i in each sample j, in the form: $effort_{ij} = \log(bias_i \times depth_j)$, where $bias_i$ is the sequencing bias correction factor for species i, estimated from our mock communities (see above, *Estimating Sequencing Bias*), and $depth_j$ is the total sum of all species in sample j, after dividing each by their species-specific sequencing bias correction factor. We used Wald tests to asses the significance of model terms, accounting for non-independence of species relative abundances by estimating a species correlation matrix [74] and by assessing significance using permutation tests, while maintaining species correlations, to calculate p-values [75]. To determine whether host ecotype explained the effects of host genotype, we fit a second multivariate glm with plant genotype re-coded as a binary factor (eastern or western).

We used two approaches to determine the relative contributions of individual species to the overall variation in community composition in response to our experimental treatments. First, we extracted univariate test statistics from our multivariate glms, using permutation tests and step-down resampling to control the family-wise error rates. To quantify univariate effect sizes, we fit individual negative-binomial glms for each species with the R-package MASS [76], and estimated the partial-R^2 for each model term, following the method of Nagelkerke [52].

As an alternative approach to assessing the impact of the experimental treatments on individual species, we quantified the benefit of preemptive colonization (i.e., priority effects) for each of the 5 initial colonists. For each initial colonist on each host genotype, we defined the strength of priority effects as the log-ratio of the mean proportional abundance when arriving first to the mean proportional abundance when arriving concurrent with the community, following [77]. This calculation results in positive values if the relative abundance was greater when the species arrived before the community. We calculated point estimates for the strength of the priority effect for each species on each host genotype, using bootstrapping to estimate confidence intervals, randomly sampling with replacement 10,000 times for each treatment combination and

recalculating the strength of the priority effect for each iteration. Bias-corrected and accelerated confidence intervals [78] were estimated from the resulting distributions. To test whether each species experienced significant priority effects on eastern or western ecotypes, we used bootstrapped one-sample t-tests. To ensure that the bootstrapping process resembled the data generation process, we used a two-stage resampling procedure, beginning with the 10,000 bootstrapped point-estimates of priority effects describe above. For each set of bootstrapped point estimates, we drew 100 bootstrap samples for each fungal species and host ecotype combination and calculated the t-statistic under the null hypothesis of no difference in relative abundance due to arrival timing. The bootstrapped, one-tailed p-values were then calculated as the proportion of times the bootstrapped t-statistics were greater than the values from the observed data.

We then tested whether our experimental treatments affected the severity of leaf rust disease, measured as the proportion of leaf surface occupied by chlorotic lesions or rust uredinia, averaged over three leaves per plant. We separated highly resistant and susceptible genotypes for this analysis because our disease severity data indicated 2 qualitatively distinct groups, one of which likely posses major-gene resistance to the rust pathogen [29,79], precluding variation in disease severity (Figures 3 & S3). For each group, we then fit generalized linear models with a beta distribution (i.e., beta-regression), using the R-package betareg [80]. To account for the presence of zeros in the rust uredinia data, a transformation was applied, following [81], $(y * (n - 1) + 0.5) / n$, where y is the proportion of leaf with rust uredinia and n is the total number of plants sampled. In addition, because some individual leaves were lost during handling, we accounted variation in measurement precision by using the number of leaves sampled per plant as proportionality weights in the models. To determine whether host genotype and fungal species arrival order interactively determined disease severity, we compared models with and without an interaction term using likelihood-ratio tests, implemented with the R-package lmtest [82]. We then tested the marginal direct effects of host genotype and species arrival order on disease severity. Analyses of both measures of rust disease severity, chlorotic lesions and uredinia, yielded identical conclusions, so we present only the former.

We then tested whether variation in disease severity within each susceptible plant genotype could be explained by variation in the relative abundance of individual foliar fungi, or community-level

variation associated with the species arrival order treatments. First, we fit a new beta-regression model to the rust severity data with only host genotype as a predictor. We then extracted the standardized residuals to use as a new response variable capturing variation in disease severity after accounting for differences among individual plant genotypes. To assess whether residual rust severity was related to the relative abundance of individual foliar fungi, we then conducted Pearson's correlation tests and examined scatter plots, using log-odds transformed proportional fungal abundance. To assess whether residual rust severity was associated with the species arrival order treatment effects on overall fungal community composition, we first conducted a distance based redundancy analysis of fungal community dissimilarity, using Jensen-Shannon Distance, and conditioned on host genotype effects, to identify orthogonal axes of variation associated species arrival order. We then used Pearson's correlation tests and examined scatter plots, as above.

All analyses were conducted using R v3.6.2 [83] and all code and raw data to reproduce the analyses has been publicly archived (http://doi.org/10.5281/zenodo.3742666).

References

1. Vandenkoornhuyse, P., Quaiser, A., Duhamel, M., Le Van, A., and Dufresne, A. (2015). The importance of the microbiome of the plant holobiont. New Phytol. *206*, 1196–1206.

2. Laforest-Lapointe, I., Paquette, A., Messier, C., and Kembel, S.W. (2017). Leaf bacterial diversity mediates plant diversity and ecosystem function relationships. Nature *546*, 145–147.

3. Cho, I., and Blaser, M.J. (2012). The human microbiome: at the interface of health and disease. Nat. Rev. Genet. *13*, 260–270.

4. Tripathi, A., Marotz, C., Gonzalez, A., Vázquez-Baeza, Y., Song, S.J., Bouslimani, A., McDonald, D., Zhu, Q., Sanders, J.G., Smarr, L., *et al.* (2018). Are microbiome studies ready for hypothesis-driven research? Curr. Opin. Microbiol. *44*, 61–69.

5. Lajoie, G., and Kembel, S.W. (2019). Making the most of trait-based approaches for microbial ecology. Trends Microbiol. *27*, 814–823.

6. Ricci, F., Rossetto Marcelino, V., Blackall, L.L., Kühl, M., Medina, M., and Verbruggen, H. (2019). Beneath the surface: community assembly and functions of the coral skeleton microbiome. Microbiome *7*, 1–10.

7. Sprockett, D., Fukami, T., and Relman, D.A. (2018). Role of priority effects in the early-life assembly of the gut microbiota. Nat. Rev. Gastroenterol. Hepatol. *15*, 197–205.

8. Moccia, K.M., and Lebeis, S.L. (2019). Microbial ecology: how to fight the establishment. Curr. Biol. *29*, R1320–R1323.

9. Kennedy, P.G., Peay, K.G., and Bruns, T.D. (2009). Root tip competition among ectomycorrhizal fungi: are priority effects a rule or an exception? Ecology *90*, 2098–2107.

10. Werner, G.D.A., and Kiers, E.T. (2015). Order of arrival structures arbuscular mycorrhizal colonization of plants. New Phytol. *205*, 1515–1524.

11. Carlström, C.I., Field, C.M., Bortfeld-Miller, M., Müller, B., Sunagawa, S., and Vorholt, J.A. (2019). Synthetic microbiota reveal priority effects and keystone strains in the *Arabidopsis* phyllosphere. Nat. Ecol. Evol. *3*, 1445–1454.

12. Martínez, I., Maldonado-Gomez, M.X., Gomes-Neto, J.C., Kittana, H., Ding, H., Schmaltz, R., Joglekar, P., Cardona, R.J., Marsteller, N.L., Kembel, S.W., *et al.* (2018). Experimental evaluation of the importance of colonization history in early-life gut microbiota assembly. Elife *7*, 1–26.

13. Palmgren, A. (1926). Chance as an element in plant geography. In Proceedings of the International Congress of Plant Sciences, B. Duggar, ed. (Ithica, New York), pp. 591–602.

14. Sutherland, J.P. (1974). Multiple stable points in natural communities. Am. Nat. *108*, 859–873.

15. Drake, J. (1991). Community-assembly mechanics and the structure of an experimental species ensemble. Am. Nat. *137*, 1–26.

16. Litvak, Y., and Bäumler, A.J. (2019). The founder hypothesis: a basis for microbiota resistance, diversity in taxa carriage, and colonization resistance against pathogens. PLoS Pathog. *15*, 1–6.

17. Dunlap, J.M., and Stettler, R.F. (2001). Variation in leaf epidermal and stomatal traits of *Populus trichocarpa* from two transects across the Washington Cascades. Can. J. Bot. *79*, 528–536.

18. Dunlap, J.M., and Stettler, R.F. (1996). Genetic variation and productivity of *Populus trichocarpa* and its hybrids. IX. Phenology and Melampsora rust incidence of native black cottonwood clones from four river valleys in Washington. For. Ecol. Manage. *87*, 233–256.

19. Dunlap, J.M., Heilman, P.E., and Stettler, R.F. (1994). Genetic variation and productivity of *Populus trichocarpa* and its hybrids. VII. Two-year survival and growth of native black cottonwood clones from four river valleys in Washington. Can. J. For. Res. *24*, 1539–1549.

20. Newcombe, G., Stirling, B., McDonald, S., and Bradshaw, H.D. (2000). *Melampsora* × *columbiana*, a natural hybrid of *M. medusae* and *M. occidentalis*. Mycol. Res. *104*, 261–274.

21. Barge, E.G., Leopold, D.R., Peay, K.G., Newcombe, G., and Busby, P.E. (2019). Differentiating spatial from environmental effects on foliar fungal communities of *Populus trichocarpa*. J. Biogeogr. *46*, 2001–2011.

22. Lindow, S.E., and Brandl, M.T. (2003). Microbiology of the phyllosphere. Appl. Environ. Microbiol. *69*, 1875–1883.

23. Vorholt, J.A. (2012). Microbial life in the phyllosphere. Nat. Rev. Microbiol. *10*, 828–840.

24. Hacquard, S., Spaepen, S., Garrido-Oter, R., and Schulze-Lefert, P. (2017). Interplay between innate immunity and the plant microbiota. Annu. Rev. Phytopathol. *55*, 565–589.

25. Jones, J.D.G., and Dangl, J.L. (2006). The plant immune system. Nature *444*, 323–329.

26. Warton, D.I., Blanchet, F.G., O'Hara, R.B., Ovaskainen, O., Taskinen, S., Walker, S.C., and Hui, F.K.C. (2015). So many variables: joint modeling in community ecology. Trends Ecol. Evol. *30*, 766–779.

27. Kainer, D., Hyatt, P.D., Jones, P., Streich, J., Shah, M., Ranjan, P., and Chen, J. (2020). The *Populus trichocarpa* pan-genome provides insights into the function of gene presence and absence variation. Nat. Genet. *In press*.

28. Zhang, B., Zhu, W., Diao, S., Wu, X., Lu, J., Ding, C., and Su, X. (2019). The Poplar pangenome provides insights into the evolutionary history of the genus. Commun. Biol. *2*, 215.

29. Duplessis, S., Major, I., Martin, F., and Séguin, A. (2009). Poplar and pathogen interactions: insights from *Populus* genome-wide analyses of resistance and defense gene families and gene expression profiling. CRC. Crit. Rev. Plant Sci. *28*, 309–334.

30. Wallace, J.G., Kremling, K.A., Kovar, L.L., and Buckler, E.S. (2018). Quantitative genetics of the maize leaf microbiome. Phytobiomes J. *2*, 208–224.

31. Ke, P.-J., and Letten, A.D. (2018). Coexistence theory and the frequency-dependence of priority effects. Nat. Ecol. Evol. *2*, 1691–1695.

32. Fukami, T., Mordecai, E.A., and Ostling, A. (2016). A framework for priority effects. J. Veg. Sci. *27*, 655–657.

33. Jumpponen, A., and Jones, K.L. (2009). Massively parallel 454 sequencing indicates hyperdiverse fungal communities in temperate *Quercus macrocarpa* phyllosphere. New Phytol. *184*, 438–48.

34. Arnold, A.E., and Lutzoni, F. (2007). Diversity and host range of foliar fungal endophytes: are tropical leaves biodiversity hotspots? Ecology *88*, 541–549.

35. Fukami, T. (2015). Historical contingency in community assembly: integrating niches, species pools, and priority effects. Annu. Rev. Ecol. Evol. Syst. *46*, 1–23.

36. Nemergut, D.R., Schmidt, S.K., Fukami, T., O'Neill, S.P., Bilinski, T.M., Stanish, L.F., Knelman, J.E., Darcy, J.L., Lynch, R.C., Wickey, P., *et al.* (2013). Patterns and processes of microbial community assembly. Microbiol. Mol. Biol. Rev. *77*, 342–356.

37. Zamioudis, C., and Pieterse, C.M.J. (2012). Modulation of host immunity by beneficial microbes. Mol. Plant-Microbe Interact. *25*, 139–150.

38. Van Wees, S.C., Van der Ent, S., and Pieterse, C.M. (2008). Plant immune responses triggered by beneficial microbes. Curr. Opin. Plant Biol. *11*, 443–448.

39. Busby, P.E., Peay, K.G., and Newcombe, G. (2016). Common foliar fungi of *Populus trichocarpa* modify *Melampsora* rust disease severity. New Phytol. *209*, 1681–1692.

40. Gloor, G.B., Macklaim, J.M., Vu, M., and Fernandes, A.D. (2016). Compositional uncertainty should not be ignored in high-throughput sequencing data analysis. Austrian J. Stat. *45*, 73.

41. Quinn, T.P., Erb, I., Richardson, M.F., and Crowley, T.M. (2018). Understanding sequencing data as compositions: an outlook and review. Bioinformatics *34*, 2870–2878.

42. Guo, X., Zhang, X., Qin, Y., Liu, Y.-X., Zhang, J., Zhang, N., Wu, K., Qu, B., He, Z., Wang, X., *et al.* (2020). Host-associated quantitative abundance profiling reveals the microbial load variation of root microbiome. Plant Commun. *1*, 100003.

43. Fukami, T. (2004). Assembly history interacts with ecosystem size to influence species diversity. Ecology *85*, 3234–3242.

44. Orrock, J.L., and Fletcher Jr., R.J. (2005). Changes in community size affect the outcome of competition. Am. Nat. *166*, 107–111.

45. Chase, J.M. (2010). Stochastic community assembly causes higher biodiversity in more productive environments. Science (80-.). *328*, 1388–1391.

46. Kardol, P., Souza, L., and Classen, A.T. (2013). Resource availability mediates the importance of priority effects in plant community assembly and ecosystem function. Oikos *122*, 84–94.

47. Leopold, D.R., Wilkie, J.P., Dickie, I.A., Allen, R.B., Buchanan, P.K., and Fukami, T. (2017). Priority effects are interactively regulated by top-down and bottom-up forces: evidence from wood decomposer communities. Ecol. Lett. *20*, 1054–1063.

48. Furches, A., Kainer, D., Weighill, D., Large, A., Jones, P., Walker, A.M., Romero, J., Gazolla, J.G.F.M., Joubert, W., Shah, M., *et al.* (2019). Finding new cell wall regulatory genes in *Populus trichocarpa* using multiple lines of evidence. Front. Plant Sci. *10*, 1–17.

49. Bodenhausen, N., Bortfeld-Miller, M., Ackermann, M., and Vorholt, J.A. (2014). A synthetic community approach reveals plant genotypes affecting the phyllosphere microbiota. PLoS Genet. *10*, e1004283.

50. Vorholt, J.A., Vogel, C., Carlström, C.I., and Müller, D.B. (2017). Establishing causality: opportunities of synthetic communities for plant microbiome research. Cell Host Microbe *22*, 142–155.

51. Christian, N., Whitaker, B.K., and Clay, K. (2015). Microbiomes: unifying animal and plant systems through the lens of community ecology theory. Front. Microbiol. *6*, 1–15.

52. Nagelkerke, N.J.D. (1991). A note on a general definition of the coefficient of determination. Biometrika *78*, 691–692.

53. Huang, Y.-L., Zimmerman, N., and Arnold, A. (2018). Observations on the early establishment of foliar endophytic fungi in leaf discs and living leaves of a model woody angiosperm, *Populus trichocarpa* (Salicaceae). J. Fungi *4*, 58.

54. Gardes, M., and Bruns, T.D. (1993). ITS primers with enhanced specificity for basidiomycetes - application to the identification of mycorrhizae and rusts. Mol. Ecol. *2*, 113–8.

55. Ihrmark, K., Bödeker, I.T.M., Cruz-Martinez, K., Friberg, H., Kubartova, A., Schenck, J., Strid, Y., Stenlid, J., Brandström-Durling, M., Clemmensen, K.E., *et al.* (2012). New primers to amplify the fungal ITS2 region–evaluation by 454-sequencing of artificial and natural communities. FEMS Microbiol. Ecol. *82*, 666–77.

56. Lundberg, D.S., Yourstone, S., Mieczkowski, P., Jones, C.D., and Dangl, J.L. (2013). Practical innovations for high-throughput amplicon sequencing. Nat. Methods *10*, 999–1002.

57. Stevens, J.L., Jackson, R.L., and Olson, J.B. (2013). Slowing PCR ramp speed reduces chimera formation from environmental samples. J. Microbiol. Methods *93*, 203–205.

58. Hamady, M., Walker, J.J., Harris, J.K., Gold, N.J., and Knight, R. (2008). Error-correcting barcoded primers for pyrosequencing hundreds of samples in multiplex. Nat. Methods *5*, 235–237.

59. Somervuo, P., Koskinen, P., Mei, P., Holm, L., Auvinen, P., and Paulin, L. (2018). BARCOSEL: a tool for selecting an optimal barcode set for high-throughput sequencing. BMC Bioinformatics *19*, 257.

60. Galanti, L., Shasha, D., and Gunsalus, K. (2017). Pheniqs: fast and flexible quality-aware sequence demultiplexing. bioRxiv, 128512.

61. Martin, M. (2011). Cutadapt removes adapter sequences from high-throughput sequencing reads. EMBnet.journal *17*, 10.

62. Sturm, M., Schroeder, C., and Bauer, P. (2016). SeqPurge: highly-sensitive adapter trimming for paired-end NGS data. BMC Bioinformatics *17*, 208.

63. Callahan, B.J., McMurdie, P.J., Rosen, M.J., Han, A.W., Johnson, A.J.A., and Holmes, S.P. (2016). DADA2: High-resolution sample inference from Illumina amplicon data. Nat. Methods *13*, 581–583.

64. Wright, Erik, S. (2016). Using DECIPHER v2.0 to analyze big biological sequence data in R. R J. *8*, 352.

65. Tuskan, G.A., DiFazio, S., Jansson, S., Bohlmann, J., Grigoriev, I., Hellsten, U., Putnam, N., Ralph, S., Rombauts, S., Salamov, A., *et al.* (2006). The genome of Black Cottonwood, *Populus trichocarpa* (Torr. & Gray). Science (80-.). *313*, 1596–1604.

66. Langmead, B., and Salzberg, S.L. (2012). Fast gapped-read alignment with Bowtie 2. Nat. Methods *9*, 357–359.

67. McMurdie, P.J., and Holmes, S. (2013). phyloseq: An R package for reproducible interactive analysis and graphics of microbiome census data. PLoS One *8*, e61217.

68. Schindelin, J., Arganda-Carreras, I., Frise, E., Kaynig, V., Longair, M., Pietzsch, T., Preibisch, S., Rueden, C., Saalfeld, S., Schmid, B., *et al.* (2012). Fiji: an open-source platform for biological-image analysis. Nat. Methods *9*, 676–682.

69. Arganda-Carreras, I., Kaynig, V., Rueden, C., Eliceiri, K.W., Schindelin, J., Cardona, A., and Sebastian Seung, H. (2017). Trainable Weka Segmentation: a machine learning tool for microscopy pixel classification. Bioinformatics *33*, 2424–2426.

70. Untergasser, A., Cutcutache, I., Koressaar, T., Ye, J., Faircloth, B.C., Remm, M., and Rozen, S.G. (2012). Primer3—new capabilities and interfaces. Nucleic Acids Res. *40*, e115–e115.

71. Lofgren, L.A., Uehling, J.K., Branco, S., Bruns, T.D., Martin, F., and Kennedy, P.G. (2019). Genome-based estimates of fungal rDNA copy number variation across phylogenetic scales and ecological lifestyles. Mol. Ecol. *28*, 721–730.

72. McLaren, M.R., Willis, A.D., and Callahan, B.J. (2019). Consistent and correctable bias in metagenomic sequencing experiments. Elife *8*, 559831.

73. Wang, Y., Naumann, U., Wright, S., and Warton, D. (2019). mvabund: statistical methods for analysing multivariate abundance data. R package version 4.0.1. URL https://CRAN.R-project.org/package=mvabund.

74. Warton, D.I. (2011). Regularized sandwich estimators for analysis of high-dimensional data using generalized estimating equations. Biometrics *67*, 116–123.

75. Warton, D.I., Thibaut, L., and Wang, Y.A. (2017). The PIT-trap—A “model-free” bootstrap procedure for inference about regression models with discrete, multivariate responses. PLoS One *12*, e0181790.

76. Venables, W.N., and Ripley, B.D. (2002). Modern Applied Statistics with S Fourth Edi. (Springer New York).

77. Vannette, R.L., and Fukami, T. (2014). Historical contingency in species interactions: towards niche-based predictions. Ecol. Lett. *17*, 115–124.

78. DiCiccio, T., and Efron, B. (1996). Bootstrap confidence intervals. Stat. Sci. *11*, 189–212.

79. Hacquard, S., Petre, B., Frey, P., Hecker, A., Rouhier, N., and Duplessis, S. (2011). The Poplar-Poplar rust interaction: insights from genomics and transcriptomics. J. Pathog. *2011*, 1–11.

80. Cribari-Neto, F., and Zeileis, A. (2010). Beta Regression in R. J. Stat. Softw. *34*, 1–24.

81. Smithson, M., and Verkuilen, J. (2006). A better lemon squeezer? Maximum-likelihood regression with beta-distributed dependent variables. Psychol. Methods *11*, 54–71.

82. Zeileis, A., and Hothorn, T. (2002). Diagnostic checking in regression relationships. R News *2*, 7–10.

83. R Core Team (2019). R: A language and environment for statistical computing. R Foundation for Statistical Computing, Vienna, Austria. URL https://www.R-project.org/.

Figure 1: Fungal species composition in the foliar microbiome depends on both species arrival order and host genotype.

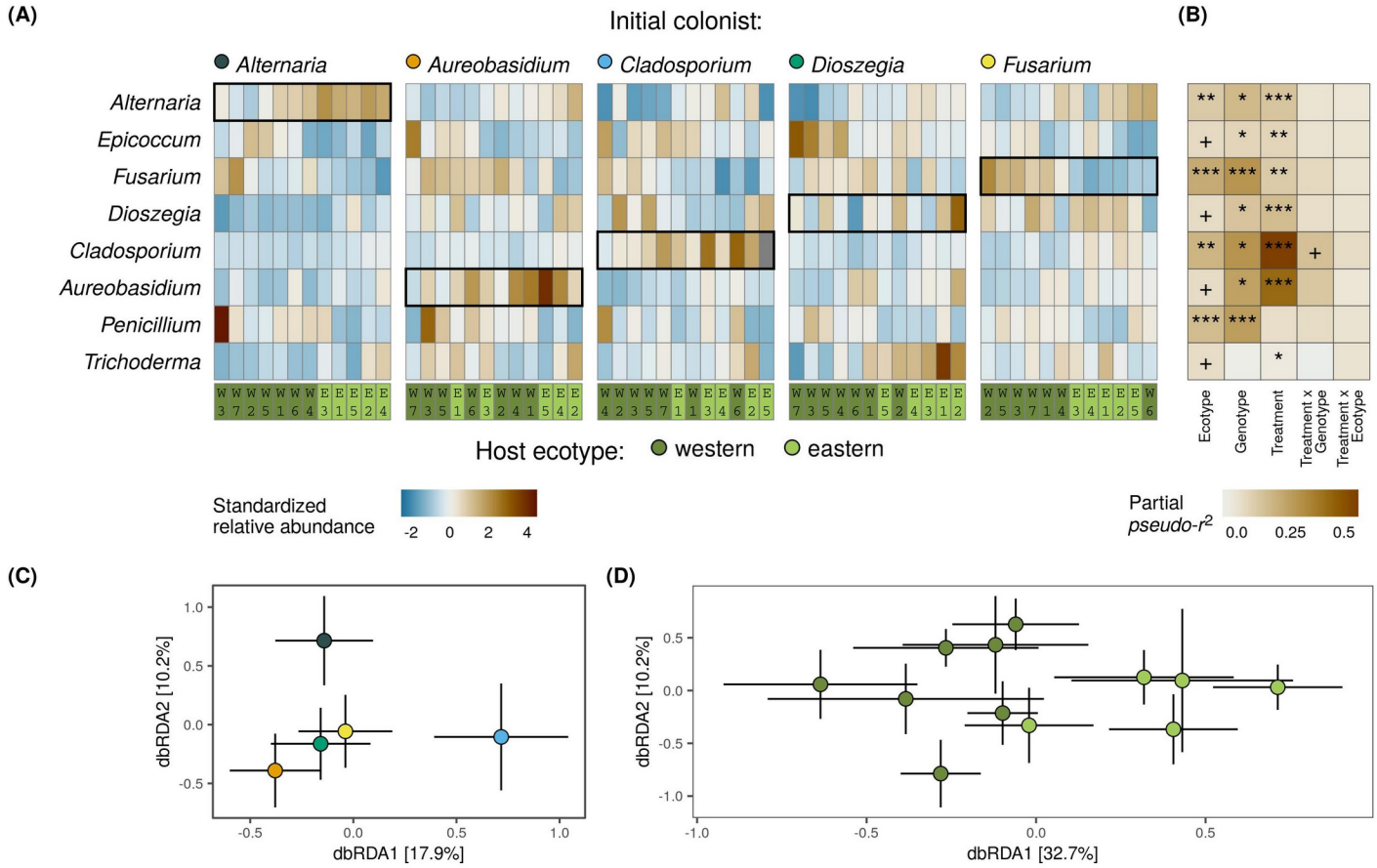

Figure 2: The advantage of preemptive colonization depends on species identity and host genotype, but not host ecotype.

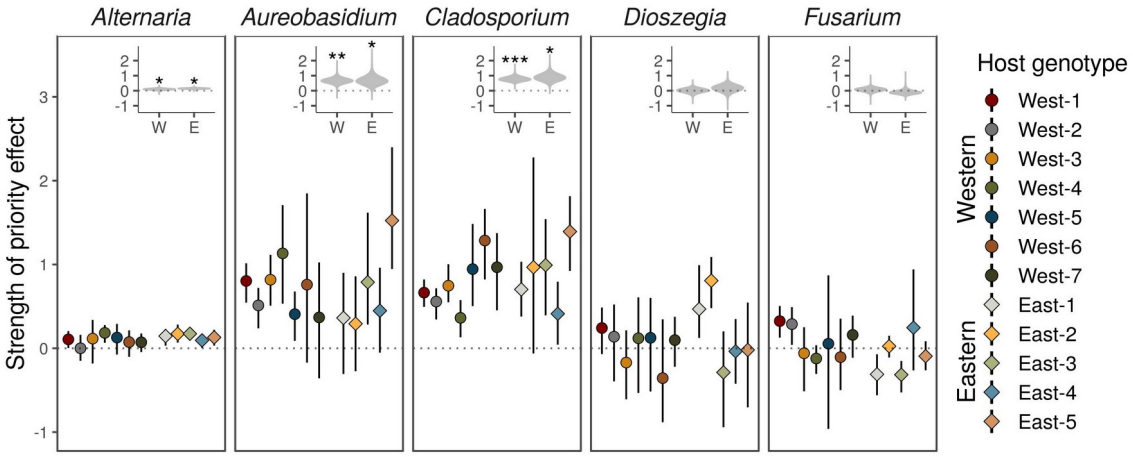
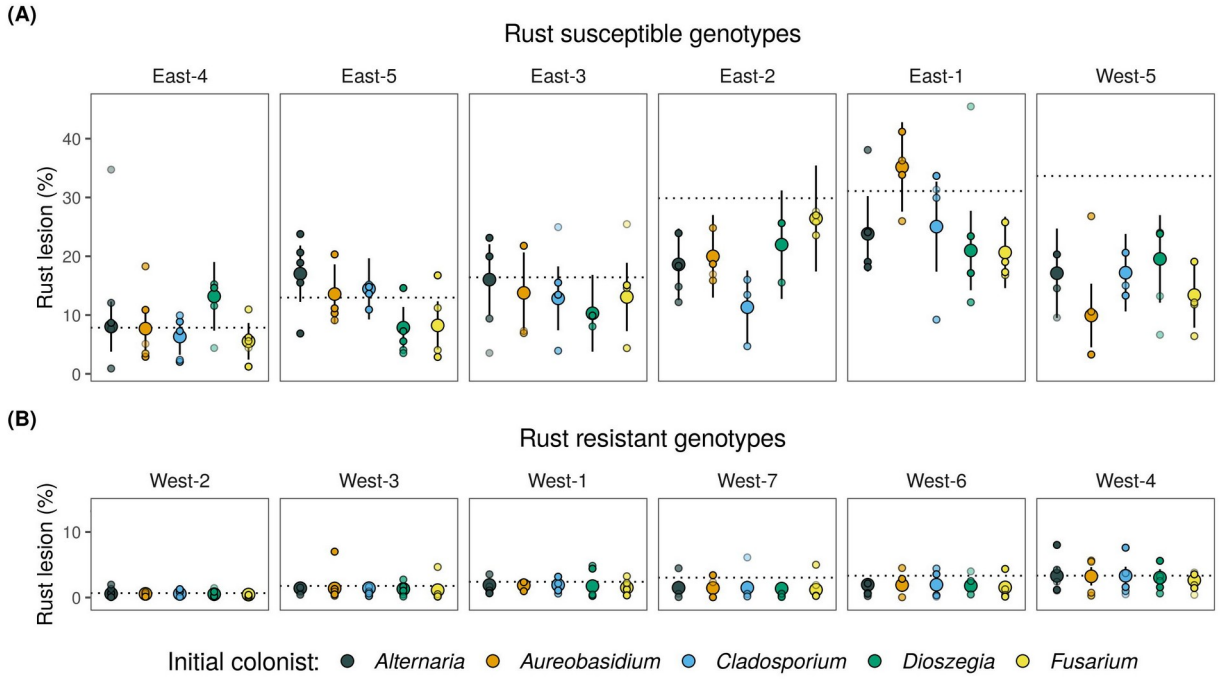
667 **Figure 3:** Foliar microbiome assembly history affects rust disease severity in susceptible plant
668 genotypes.